An Iterative Stochastic Approach to Constrained Drones' Communications

Giovanni Iacovelli*§, Pietro Boccadoro†§, Luigi Alfredo Grieco‡§,
Department of Electrical and Information Engineering (DEI), Politecnico di Bari, Bari, Italy
§CNIT, Consorzio Nazionale Interunivesitario per le Telecomunicazioni, Bari
Email: giovanni.iacovelli@poliba.it*, †pietro.boccadoro@poliba.it, ‡alfredo.grieco@poliba.it,

***Abstract*—The Internet of Drones paradigm is considered as a key enabler for several cutting edge verticals, including surveillance, planetary exploration, protection, loads transportation, and aerology. The main limitations to its wide-scale adoption arise from the constraints on the resources available onboard of drones: this concerns energy, computational and storage capabilities. Unfortunately, current literature mainly focuses on energy limitations, leaving unexplored the interplay with other constraints. To bridge this gap, the present contribution also encompasses the limitations on the memory onboard, which can be critical when drones have to acquire high resolution multimedia signals for ambient awareness services. In particular, an iterative stochastic approach is conceived hereby to tune data flows from/to drones subject to energy and memory constraints in order to fulfill an Out-of-Service probability below a given threshold. Stemming from the proposed approach, two algorithms have been also designed that seek a different complexity-performance tradeoff. The first one is less complex and more conservative, since it plans the mission once at the beginning. The second, instead, is slightly more complex and aggressive but it allows the drone to gather and upload a higher volume of data and shorten the gap with respect to the ideal case.**

***Index Terms*—Data communications, Mobile environments, Modeling Techniques, Internet of Drones.**

I. Introduction

The Internet of Drones (IoD) is a network architecture specifically designed to leverage the huge potential of Unmanned Aerial Vehicles (UAVs) [1]. This is motivated by the many features that drones expose by design, such as their high degree of mobility in arbitrary 3D environments and the ability to: gather data coming from the Internet of Things (IoT), move variable payloads, survey wide areas of interest [2], and serve as flying Base Stationss (BSs) in 6G & beyond systems [3], [4]. Despite their huge potential, UAVs may suffer from limitations in terms of maximum weight transport, mission endurance, and cruise speed. Some of those restrictions may critically interplay, thus requiring dedicated optimization strategies.

Drones' flight has been extensively analyzed from different perspectives: (i) energy consumption related to drones' movements [5]–[7], (ii) path optimization [7], [8], (iii) communication links and reliability [2], [9], (iv) coverage area [2], (v) mission duration [10], [11], [14], and (vi) optimal data gathering [12]. The joint resolution of those issues has been formulated in [13]–[15] as optimization problems. Despite the scientific literature, to the best of authors' knowledge, the solutions proposed so far did not consider at all the constraints related to onboard memory availability and almost exclusively deal with energy limitations while tackling mission planning and/or trajectory design. Unfortunately, memory constraints are no longer negligible in missions targeting continuous monitoring or acquisition of high resolution multimedia signals, such as coastline erosion or crop monitoring [16]–[18].

This work investigates a continuous acquisition scenario in which a drone gathers high resolution videos and, to raise the responsiveness of the monitoring service, delivers low-quality versions of gathered data to the reference ground infrastructure. Known the harmonization perspective of 6G, the existing cellular network infrastructure could be empowered by supporting multiple technologies, such as Visible Light Communications (VLC). Therefore, it is assumed that BSs will be way-points composing the mission plan, functionally endowed with VLC receivers, and, from now on, referred to as Check-Points (CPs). This surveying activity implies a certain energy consumption, due to mechanical and data gathering operations. It is worth to note that mechanical energy spent over the mission is not known in advance and the amount of data to acquire is subjected to memory availability constraints. Therefore a sophisticated approach is required to tune the incoming/outgoing data streams from/to drones to/from CP with the aim of maximizing the total amount of gathered/uploaded data while lowering the probability to run out of energy before the mission is completed. Before the mission starts, an *a priori* tuning of incoming/outgoing flows is planned based on a stochastic approach that targets an Out-of-Service probability below a given threshold ε. As a matter of fact, these allocations may be too conservative. Hence, an Iterative Stochastic ApproAch to constrained drones' Communications, namely ISAAC, is also proposed hereby that: (1) models the mechanical energy required over the mission as a random variable, (2) provides an initial setting for the amount of data to gather/upload over the mission in order to keep the Out-of-Service probability below a given threshold ε, and (3) refines settings out of point (2), based on the actual memory and energy availabilities measured during the mission. To analyze the performance of the proposed approaches (i.e., the *a priori* algorithm and *ISAAC*) a thorough simulation campaign has been carried out in a wide set of scenarios and with respect to an ideal solution,i.e. *a posteriori*, that plans the mission

978-1-7281-7343-6/20/$31.00 ©2020 IEEE

knowing in advance the exact value of the mechanical energy expenditure. Simulation results show that: (i) both algorithms provide the same performance of the ideal one for a relatively low number of CPs, (ii) *ISAAC* remarkably outperforms the *a priori* approach in scenarios with a relatively high number of BSs.

The remainder of this work is as follows: Section II defines the reference scenario/mission. With Section III, a through formulation of the envisioned problem is given. Section IV presents the approaches to properly introduce Section V, which, in turn, analyses the numerical results. Finally, Section VI concludes the work drawing future possibilities.

II. Reference Scenario

The reference scenario involves a drone that takes off from a base starting point, meets N CPs, and, finally, returns to the starting point. Accordingly, the mission is a sequence of segments, each one bounded by two consecutive CPs, with the sole exception of the first (from the starting point to the first CP) and the last segments (from the last CP back to the starting point). During the flight, the drone is assumed to acquire high-resolution images and videos, an operating assumption that is of relevance in both military and civil applications [2].

Ideally, as soon as the drone meets a CP, acquired information are uploaded to it and the process is iterated until the end of the mission. Assuming to use User Datagram Protocol (UDP) for uploading operations, offloading of transmitted data is avoided in order to keep a high resolution version of data onboard while speeding up data transmission. In real world scenarios, the flight of the drone is subject to a number of standing in conditions, such as constrained energy and onboard memory availabilities. As for energy, drones are battery-powered systems, thus requiring dedicated utilization policies. On the overall energy consumption, flight mechanics accounts for an unavoidable, still relevant, quota, which may become of great relevance in close relation to attitude/elevation variations, as well as adverse weather conditions. In addition, image acquisitions and data upload operations have relevant effect on energy consumption, especially in presence of high resolution images/videos, thus immediately affecting memory usage and the responsiveness of the monitoring service running on top of the UAV. Therefore, a critical tradeoff arises when energy and memory constraints interplay with responsiveness requirements of the mission. In order to tune the amount of data to acquire on each segment of the mission and to upload at each CP, given the constraints on energy and memory

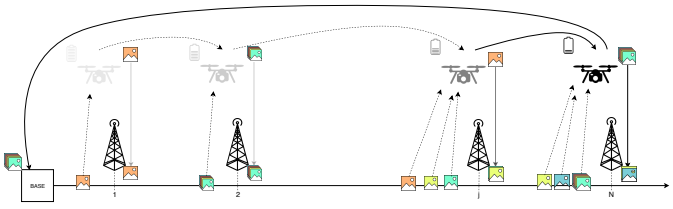

Fig. 1: Reference scenario with a drone during the mission.

Symbol	Description
N	Number of Check-Points
E_0	Initial amount of energy available on board
E_j	Energy available on board when the drone approaches the j-th CP
k_1,k_2	Proportionality coefficients to account for the energy spent in upload and acquisition operations [J/GB]
E_{D_j}	Random variable modeling mechanical-related energy spent across the j-th segment
E_T	Random variable modeling energy needed to face the last segment of the mission
M_∞	Onboard available memory
o_j	Data quantity to upload at j-th CP
i_j	Data quantity to acquire along the j-th segment of the mission
μ_{D_j}	First order statistical moment of E_{D_j}
μ_T	First order statistical moment of E_T
σ_D	Standard deviation of E_D
σ_T	Standard deviation of E_T

TABLE I: Summary of Notation.

availability at the beginning of each segment, an iterative stochastic approach is defined hereby. In Table I, the notation used within the present work is outlined.

The key assumptions of the proposed approach are:

- The amount of mechanical energy spent across the j-th segment of the mission is a random variable E_{D_j} with mean μ_{D_j} and variance $\sigma^2_{D_j}$ with $j \in [1, N]$. Moreover, the energy required to revert to the starting point after the last CP has been met is a random variable E_T with mean μ_T and variance σ^2_T. Those assumptions reflect the fact that the energy spent on each segment cannot be known in advance because during the mission the drone has to continuously control its operations based on unforeseeable surrounding conditions (i.e., physical and/or environmental) shaped by the confidence interval. Furthermore, those random variables are assumed independent from each other.
- The amount of data gathered along the j-th segment (i.e., i_j) is proportional to μ_{D_j}. The motivation behind this assumption is that the longer the segment, the larger the amount of data that will be acquired. Moreover, the longer the segment, the larger μ_{D_j}. As a consequence, it holds
$$\frac{i_j}{i_h} = \frac{\mu_{D_j}}{\mu_{D_h}} \forall j, h \in [1..N]. \quad (1)$$
.
- The amount of data o_j uploaded at the j-th CP is proportional to the amount of data i_j gathered along the j-th path:
$$o_j = \alpha i_j. \quad (2)$$
with $0 \leq \alpha \leq 1$ This assumption models the upload of a low resolution version of the contents gathered along the j-th segment, based on scalable quality encoding [19].
- The energy spent in data uploads (from the drone to the CPs) operations is proportional to the amount of uploads data through the constant k_1.
- The energy spent in the acquisition operations is proportional to the amount of gathered data through the constant k_2.

The goal of this manuscript is to define an algorithm that tunes the values of o_j and i_j (with $1 \leq j \leq N$) in order to successfully complete the mission without violating energy and memory constraints.

III. Iterative Stochastic Approach to the Mission

With respect to the scenario described in Section II, the following theorem grounds the iterative stochastic approach proposed hereby. In particular, it states how to set i_k and o_k (with $j \leq k \leq N$) once the j-th CP is approached in order to keep the Out-of-Service probability below a given threshold ε without violating energy constraints. In particular, the following requirements will be considered:

Requirement 1: *Once the N-th CP is reached, the energy available onboard E_N should be larger than the energy required to revert back to the starting point with probability greater than $1-\varepsilon \Leftrightarrow P_r(E_N < E_T) \leq \varepsilon$.*

Requirement 2: *Once the j-th CP has been approached, the values of i_k with $k \in [j....N]$ should be set in order to avoid a memory overflow $\sum_{k=j}^{N} i_k \leq M_\infty - \sum_{l=1}^{j-1} i_l$.*

Theorem 1. *Knowing the values E_{D_l}, i_l, and o_l with $1 \leq l \leq j-1$ and assuming that E_{D_k} with $j \leq k \leq N$ and E_T are Gaussian independent random variables, Requirements 1 and 2 are satisfied if and only if*

$$i_j \leq \frac{\mu_{D_j}}{\sum_{k=j}^{N} \mu_{D_k}} \cdot \Omega_j \quad \forall j \in [1..N]. \tag{3}$$

where

$$\zeta = M_\infty - \sum_{l=1}^{j-1} i_l. \tag{4}$$

$$\xi = \frac{E_{j-1} - \gamma_{j-1}}{k_1\alpha + k_2}. \tag{5}$$

$$\Omega_j = min\left(\zeta, \xi\right). \tag{6}$$

$$E_{j-1} = E_0 - \sum_{l=1}^{j-1} E_{D_l} - k_1 \sum_{l=1}^{j-1} o_l - k_2 \sum_{l=1}^{j-1} i_l. \tag{7}$$

$$\gamma_j = Q_j^{-1}(\varepsilon). \tag{8}$$

provided that $E_j - \gamma_j \geq 0 \quad \forall j \in [1, N-1]$
being $\mu_{TD_j} = \mu_T + \sum_{k=j}^{N} \mu_{D_k}$, $\sigma_{TD}{}_j^2 = \sigma_T^2 + \sum_{k=j}^{N} \sigma_{D_k}^2$, and $Q_j(x) = \frac{1}{\sqrt{2\pi}} \int_{\frac{x-\mu_{TDj}}{\sigma_{TD_j}}}^{+\infty} e^{-\frac{t^2}{2}} dt$

Proof. At takeoff, the drone is supposed to be fully charged. As the mission starts, it steers at the first CP, while surveying (i.e., acquiring video images) the fly over area. At the N-th CP, the residual energy must be sufficient to sustain the last segment of the mission, back to starting point. When the UAV has reached the N-th CP, the remaining amount of energy can be expressed as:

$$E_N = E_0 - \sum_{k=1}^{N} E_{D_k} - k_1 \sum_{k=1}^{N} o_k - k_2 \sum_{k=1}^{N} i_k. \tag{9}$$

Hence, it is possible to state that the probability that the leftover energy is less than E_T must be as low as ε.

$$P_r(E_N < E_T) \leq \varepsilon \tag{10}$$

which is equivalent to:

$$P_r(E_T + \sum_{k=1}^{N} E_{D_k} > E_0 - k_1 \sum_{k=1}^{N} o_k - k_2 \sum_{k=1}^{N} i_k) \leq \varepsilon$$

Since, it is possible to consider $E_{D_k} \sim N(\mu_{D_k}, \sigma_{D_k}^2)$ and $E_T \sim N(\mu_T, \sigma_T^2)$, it results that:

$$E_{TD_1} = E_T + \sum_{k=1}^{N} E_{D_k}. \tag{11}$$

$$E_{TD_1} \sim N\left(\mu_T + \sum_{k=1}^{N} \mu_{D_k}, \sigma_T^2 + \sum_{k=1}^{N} \sigma_{D_k}^2\right).$$

The probability value of interest is associated with an event that happens with low probability (i.e., on the Gaussian's tail), which leads the study to include the Q-function. Unfortunately, E_{TD_1} is not a normal standard distribution. The Q-function is defined as follows:

$$Q(\gamma_0) = \varepsilon \tag{12}$$

being γ_0 the value that maximises the Out-of-Service probability. With a simple change of notation, it results:

$$Q_1(x) = Q(\frac{x - \mu_{TD_1}}{\sigma_{TD_1}}) \tag{13}$$

from which it can be derived:

$$Q_1^{-1}(\varepsilon) = \gamma_0. \tag{14}$$

Therefore, it is possible to write:

$$k_1 \sum_{k=1}^{N} o_k + k_2 \sum_{k=1}^{N} i_k \leq E_0 - \gamma_0. \tag{15}$$

Further, the amount of occupied memory cannot exceed the maximum amount of memory available, which implies:

$$\sum_{k=1}^{N} i_k \leq M_\infty. \tag{16}$$

Based on (2)

$$(k_1\alpha + k_2) \sum_{k=1}^{N} i_k \leq E_0 - \gamma_0$$

$$\sum_{k=1}^{N} i_k \leq \frac{E_0 - \gamma_0}{(k_1\alpha + k_2)}. \tag{17}$$

Now, it is possible to combine (16) and (17) to write:

$$\Omega_1 = min\left(M_\infty, \frac{E_0 - \gamma_0}{k_1\alpha + k_2}\right) \tag{18}$$

and, thanks to (1), it results:

$$i_1 = \frac{\mu_{D_1}}{\sum_{k=1}^{N} \mu_{D_k}} \Omega_1. \tag{19}$$

Once the UAV has reached the 1-st CP, the remaining amount of energy can be expressed as:

$$E_1 = E_0 - E_{D1} - k_1 o_1 - k_2 i_1 \tag{20}$$

The proposed approach can be considered as iterative and, hence, it is possible to calculate what happens at the 2-nd CP. In particular, once defined E_1 in (20), it is possible to reformulate (10) as:

$$P_r(E_N < E_T) \leq \varepsilon$$
$$P_r(E_T + \sum_{k=2}^{N} E_{D_k} > E_1 - k_1 \sum_{k=2}^{N} o_k - k_2 \sum_{k=2}^{N} i_k) \leq \varepsilon$$

It is worth remarking that being E_{D_1} known, so it is in Equation (20), and it is possible to derive E_{TD_2} as:

$$E_{TD_2} = E_T + \sum_{k=2}^{N} E_{D_k}$$
$$E_{TD_2} \sim N\left(\mu_T + \sum_{k=2}^{N} \mu_{D_k}, \sigma_T^2 + \sum_{k=2}^{N} \sigma_{D_k}^2\right)$$

Once again, it is mandatory to calculate the γ_1 corresponding to the new distribution E_{TD}:

$$Q(\gamma_1) = \varepsilon$$
$$Q_2(x) = Q(\frac{x - \mu_{TD_2}}{\sigma_{TD_2}})$$
$$Q_2^{-1}(\varepsilon) = \gamma_1.$$

The new energy constraint is:

$$k_1 \sum_{k=2}^{N} o_k + k_2 \sum_{k=2}^{N} i_k \leq E_1 - \gamma_1$$

which, based on (2), is equivalent to:

$$(k_1\alpha + k_2) \sum_{k=2}^{N} i_k \leq E_1 - \gamma_1$$

thus leading to:

$$\sum_{k=2}^{N} i_k \leq \frac{E_1 - \gamma_1}{(k_1\alpha + k_2)} \tag{21}$$

whereas, the memory constraint can be expressed as follows:

$$\sum_{k=2}^{N} i_k \leq M_\infty - i_1. \tag{22}$$

Since our aim is to maximize the memory output, lowering the amount of energy intake, it can be written:

$$\Omega_2 = min\left(M_\infty - i_1, \tfrac{E_1 - \gamma_1}{k_1\alpha + k_2}\right) \tag{23}$$

from which can be obtained:

$$i_2 = \frac{\mu_{D_2}}{\sum_{k=2}^{N} \mu_{D_k}} \Omega_2 \tag{24}$$

The same rationale can be used to demonstrate the theorem for any value of j. ■

To apply Theorem 1 in real settings it is necessary to define α. In the following remark a rationale to iteratively set α is proposed:

Remark 1. *At the j-th CP, three possible cases (Figure 2) may be verified:*

***Case A**: the energy constraint always dominates over the memory one (i.e., (4) is greater than (5), which means $\zeta > \xi$) $\forall\alpha$, which implies an optimal value of $\alpha = 0$, to maximize*

$$\Omega_j = \frac{E_{j-1} - \gamma_{j-1}}{k_2} \tag{25}$$

***Case B**: the memory constraint dominates over the energy one (i.e., (5) is greater than (4), which means $\xi > \zeta$) $\forall\alpha$, which implies an optimal value of $\alpha = 1$ that maximizes the responsiveness. In this case, Ω_j is expressed as*

$$\Omega_j = M_\infty - \sum_{l=1}^{j-1} i_l \tag{26}$$

***Case C**: in this case, ζ and ξ intersect at $\alpha = \alpha^*$, which is the optimum value to maximize $\sum_{l=1}^{N} i_l$ and $\sum_{l=1}^{N} o_l$. Hence, Ω_j can be expressed as*

$$\Omega_j = min\left(\underbrace{M_\infty - \sum_{l=1}^{j-1} i_l}_{\zeta}, \underbrace{\frac{E_{j-1} - \gamma_{j-1}}{k_1\alpha + k_2}}_{\xi}\right)$$

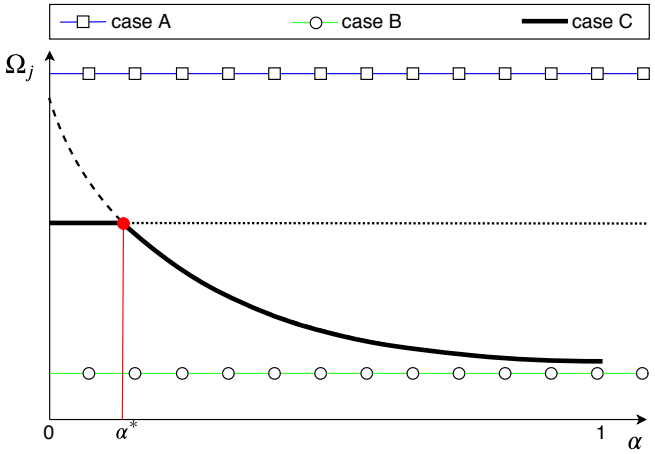

Fig. 2: Cases and combination of memory occupancy as a function of α.

Corollary 1. *Without loss of generality, the hypothesis that E_{D_j} and E_T distributions are Gaussian may not be strictly verified. In this case, E_{TD_j} will not be Gaussian. Therefore, it is possible to define F_{D_j} and F_T as the distributions associated to the random variables E_{D_j} and E_{TD_j}. The only required changes are the definition of γ, which is now equal to $F_{C_j}^{-1}(\varepsilon)$ is the Complementary Cumulative Distribution Function definition of E_{TD_j}.*

IV. The proposed Algorithms

According to the mathematical formulation proposed in Theorem 1, three approaches are possible.

The first one is an iterative solution (namely, *ISAAC*) that introduces continuous refining of the involved parameters, hence regulating data acquisition as a function of the amount of energy used by the drone during the mission each time a CP is approached. The second, instead, is more conservative and less complex approach, namely *a priori*, to compute acquired/uploaded data amounts (e.g., i_j and o_j), for each CP, just once, at the beginning of the mission. Here, the value of Ω is kept equal to the one calculated at the starting point (i.e., $\Omega = \Omega_1$). Last approach, called *a posteriori*, uses the actual values of mechanical energy consumption, leveraging the above reported equations. Such a solution is equivalent to deal with the problem from a deterministic point of view, since it is equivalent to evaluate the reference parameters at the end of the mission. It is reasonable to assume that: (i) *ISAAC* can provide a more aggressive behaviour when compared to the *a priori* algorithm, (ii) the comparison with *a posteriori* benchmarking algorithm is useful to evaluate the improvement that *ISAAC* can provide.

A. Computational Complexity

An estimation has been carried out on the proposed solutions, e.g., *a priori* and *ISAAC* algorithms. A detailed outlook on the involved operations is reported in Table II. Figure 3 compares the complexity of the two approaches as a function of the number of CPs: as expected, the *a priori* approach can be useful in those scenarios characterized by very low complexity requirements, whereas *ISAAC* needs larger computing resources. At the same time, it is worth to note that the computing load due to *ISAAC* is distributed over the N CPs and therefore it is sustainable.

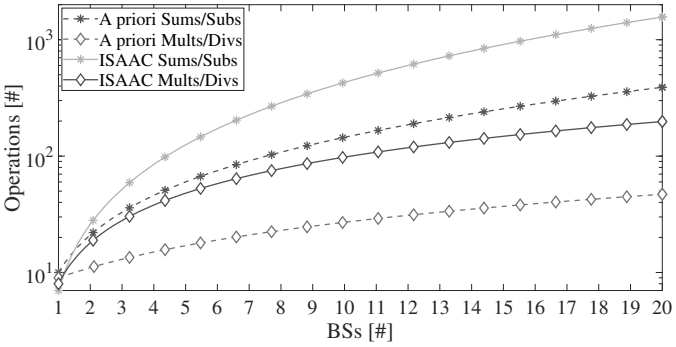

Fig. 3: Computational Complexity Analysis of the *a priori* and *iterative* algorithms.

	A priori	*ISAAC*
Sums/Subtractions	$\frac{1}{2}(N^2+19N))$	$\frac{1}{2}(7N^2+17N-10)$
Multiplications/Divisions	2N+7	2(5N-1)

TABLE II: Computational Complexity of proposed algorithms.

V. Performance evaluation

In this Section, the *ISAAC* algorithm is compared with *a priori* and *a posteriori* algorithms. A wide simulation campaign has been carried out to analyze the performance of *ISAAC* in a broad range of settings. A Monte Carlo Matlab-based simulator has been developed to compare the different algorithms. For each simulation settings, 10^5 runs have been carried out. For all the results presented in Section V-B, the average values and standard deviation have been reported for each algorithm/scenario. The main assumptions of the simulation model are described in Section V-A.

A. Simulation Settings

All the parameters involved in the simulation campaign are widely discussed hereby and their reference values are summarized in Table III.

Variable	Input/Output	Values
N	I	[1, 7] [#]
N_{MAX}	I	7 [#]
$U_1 : 3\sigma_D$	I	$10\%\mu_D$
$U_2 : 3\sigma_D$	I	$20\%\mu_D$
ε_1	I	1 [%]
ε_2	I	2 [%]
Onboard Memory	I	128, 1024, 2048 [GB]
i	O	[GB]
o	O	[GB]
$\sum_{j=1}^{N} i_j$	O	[GB]
Available Energy	O	[J]
Available Memory	O	[GB]

TABLE III: Input and Output simulation parameters.

1) Scenarios description: Two scenarios have been considered: the first is a urban setting (i.e., densely populated environment) whereas the second is a rural one. The main difference between them is the inter-CPs distance, which is of 200 m, in the first case, and 1732 m in the second [23]. For both, the distances are calculated as a random variable uniformly distributed with a range of $\pm 10\%$. In the urban scenario, the maximum number of CPs has been set to $N_{MAX} = 74$, which guarantees that the energy onboard is always lower than the mechanical energy required for the mission. In the rural case, instead, the maximum number of CPs is $N_{MAX} = 7$. For instance, according to [22], E_0 has been set to 213.4 kJ. Moreover, two different values of the confidence interval for the mechanical energy have been herein considered, e.g., 10% and 20%. All the results that will be presented later on in this Section will be related to the rural case. The results related to the urban scenario are very similar with the only difference of involving a larger number of CPs.

2) Power consumption model: This work uses the model proposed in [5] to characterize the average mechanical power $P(V)$ spent by a drone flying at speed V:

$$P(V) = P_0\left(1+\frac{3V^2}{U_{tip}^2}\right) + P_i\left(\sqrt{1+\frac{V^4}{4v_0^4}}-\frac{V^2}{2v_0^2}\right)^{1/2} + \frac{1}{2}d_0\rho s A V^3 \quad (27)$$

which is composed by the blade profile power (i.e., P_0) and the induced power in hovering status (i.e., P_i).

3) Memory Configuration: To verify the model's reliability, the drone has been supposed to be equipped with three onboard memory capabilities, i.e., 128 GB, 1024 GB, and 2048 GB. In the first case, memory is a major concern in terms of resource handling, whereas, in the second one, both memory and energy availabilities are likely to be sufficient to successfully handle the mission. Lastly, in the third configuration, energy becomes the priority.

4) Data-to-Energy constants definition: The energy amount employed for the transmission of the acquired data toward the CP is strongly connected to the involved technology. In this case, drones are assumed to communicate thanks to a 5G infrastructure. The energy consumption can be assumed as 2.3 nJ/bit [20], which leads to $k_1 \simeq 19.76$ J/GB. The drone is herein assumed to enrol an Intel RealSense D430 camera [21], with a resulting power consumption equal to 3.5 W. The value of k_2 has been calculated as the ratio between the power consumption of the camera used by the drone to acquire both the Red Green and Blue (RGB) and Depth data and the value resulting from the summation of all data fluxes, i.e., aggregated flux. Assuming an RGB 1920x1080 resolution with 2 B/px depth @30 fps, the resulting throughput is 118.65 MB/s. With a 848x480 resolution @90 fps for the Depth, the resulting throughput is 69.87 MB/s. Therefore, with 2 B/px, the overall throughput is 180.52 MB/s, or 0.1841 GB/s, from which it results that k_2 is equal to 19 J/GB.

5) Out-of-Service Probability: The Out-of-Service probability ε in **Requirement 1** is set to either 1% or 2%.

B. Simulation Results

Table IV shows the Out-of-Service frequency in the considered scenario. In the 128 GB case, no outage has been measured because in this memory configuration, at any moment, the memory constraint dominates over the energy-related one. The whole memory amount is filled up during the mission with a rate that results be fairly proportional to the length of each segment. Both acquired and uploaded memory occupancies demonstrated a constant trend. Furthermore, all considered algorithms behave the same under this configuration, so that the rest of the Section will focus on 1024 and 2048 GB settings. For the ideal *a posteriori* algorithm, no outage is measured because the mission is planned based on real mechanical energy consumption values, which are supposed to be known in advance. On the other side, both *a priori* and *ISAAC* provide similar Out-of-Service frequencies, in the worst case, extremely close to the theoretical bounds (ε_1, and ε_2).

1) 1024 GB configuration: Figures 4a and 4b show the total acquired and uploaded data, respectively, in a scenario with 7 CPs, under different parameter settings. The total acquired data is almost the same whatever the algorithm and/or the simulation settings because the amount of onboard memory is limited and, as a such, all algorithms acquire an amount of data which is very close to 1024 GB. Differently from the total acquired data, the total uploaded data in the *a priori* approach is remarkably lower than using *ISAAC* or the ideal *a posteriori* solution. In addition, *ISAAC* grants a better performance level with respect to the *a priori* solution, closer to the ideal *a posteriori* algorithm. Figures 5a and 5b show the total acquired and uploaded data at each CP over the mission, respectively. Again, no remarkable differences are observed for the acquired data across the different algorithms/simulation settings. Once again, this is motivated by the fact that the memory onboard is limited and all algorithms set the amount of data to acquire to 1024 GB over 7 CPs. The uploaded data at each CP is almost constant for the *a priori* and the *a posteriori* algorithms but progressively increases from one CP to the next one when *ISAAC* is used. Similar outcomes have been observed in all other configurations.

2) 2048 GB configuration: In this configuration, the amount of onboard memory is no longer limited and the iterative algorithm, acquires an amount of data which is very close to the available amount. The *a posteriori* benchmarking solution maximises the amount of acquired memory, whereas the *a priori* solution confirms its conservative trend (see Figures 6a and 6b). The total uploaded data, instead, in the *a priori* approach is remarkably lower when compared to *ISAAC*. The spread among the values is confirmed with reference to the ideal *a posteriori* solution. Figures 7a and 7b show the total acquired and uploaded data at each CP over the mission, respectively. The *a priori* algorithm demonstrates its conservative behaviour which is, at the beginning of the mission, emulated by *ISAAC* that starts to refine the acquired amount of data, getting closer to the theoretical *a posteriori* solution. At the end of the mission, the acquired data results to be sensibly higher when compared to the ideal behaviour, thus demonstrating its added value. Even for the uploading, *ISAAC* shows the increasing gain trend which implies that the amount of uploaded data is significantly higher at the end of the mission when compared with *a priori* solution, heading to ideal values. Similar outcomes have been observed also in other configurations.

VI. Conclusions

This work discussed an iterative stochastic approach to the prototypical mission of a drone surveying a certain area, gathering high quality video data and uploading low quality versions of those data through a set of CPs along the path. During the mission, the drone is subject to constraints related to energy and memory availabilities. Starting from the proposed approach, two algorithms have been conceived that seek different complexity-performance tradeoffs. The two, namely *a priori* and *ISAAC*, respectively, were compared to an ideal solution that knows in advance the actual energy spent on each segment of the mission. Simulation results show that, in relatively short missions, all algorithms behave the same. As the mission length increases, *ISAAC* provides a performance level closer to the ideal solution than the *a priori* algorithm. Despite the relevance of the findings, future perspectives remain open. First of all, the reference mission can be carried out by a swarm of drones, thus implying flight coordination

	BSs	1024 GB												2048 GB											
		A priori				Iterative				A posteriori				A priori				Iterative				A posteriori			
		U_1		U_2		U_1		U_2		U_1		U_2		U_1		U_2		U_1		U_2		U_1		U_2	
		ε_1	ε_2	ε_1	ε_2	ε_1	ε_2	ε_1	ε_2	ε_1	ε_2	ε_1	ε_2	ε_1	ε_2	ε_1	ε_2	ε_1	ε_2	ε_1	ε_2	ε_1	ε_2	ε_1	ε_2
Rural	**1**	0	0	0	0	0	0	0	0	0	0	0	0	0	0	0	0	0	0	0	0	0	0	0	0
	2	0	0	0	0	0	0	0	0	0	0	0	0	0	0	0	0	0	0	0	0	0	0	0	0
	3	0	0	0	0	0	0	0	0	0	0	0	0	0.006	0.011	0.009	0.018	0.004	0.006	0.005	0.01	0	0	0	0
	4	0	0	0	0	0	0	0	0	0	0	0	0	0.01	0.019	0.01	0.02	0.01	0.02	0.01	0.02	0	0	0	0
	5	0	0	0	0	0	0	0	0	0	0	0	0	0.01	0.02	0.01	0.021	0.01	0.02	0.01	0.02	0	0	0	0
	6	0.01	0.018	0.01	0.02	0.005	0.011	0.005	0.01	0	0	0	0	0.01	0.019	0.01	0.02	0.01	0.02	0.01	0.019	0	0	0	0
	7	0.01	0.02	0.01	0.02	0.01	0.02	0.01	0.02	0	0	0	0	0.01	0.021	0.01	0.02	0.01	0.02	0.01	0.021	0	0	0	0

TABLE IV: Out-of-Service frequency measured in the experimental campaign.

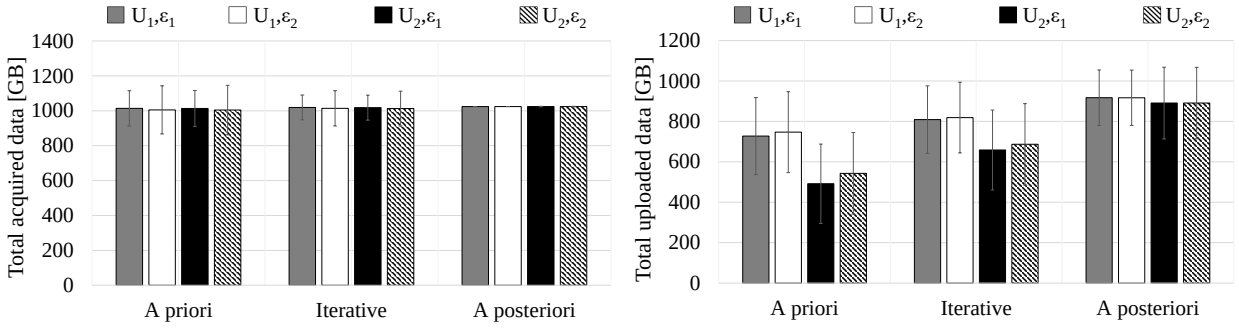

(a) Total acquired data. (b) Total uploaded data.

Fig. 4: Acquired and uploaded data in the 1024 GB configuration.

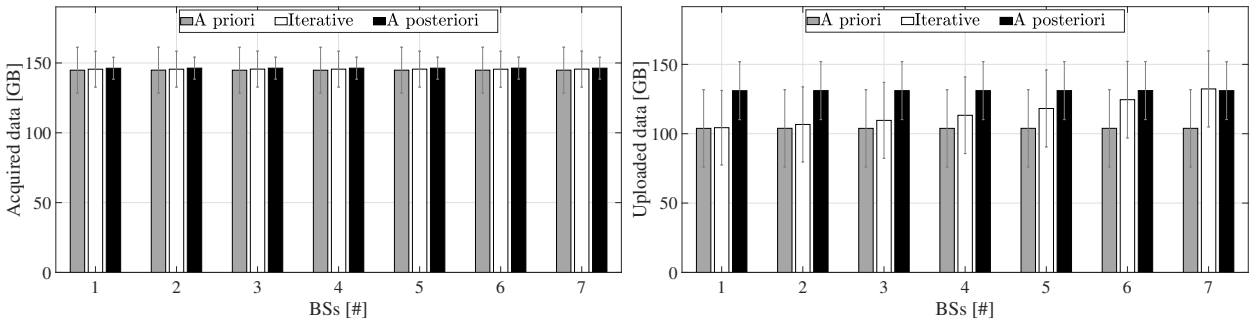

(a) Acquired data over each segment of an 7 CPs-long mission. (b) Uploaded data over each segment of an 7 CPs-long mission.

Fig. 5: Approaches comparison in the 1024 GB configuration, with U_1, and ε_1.

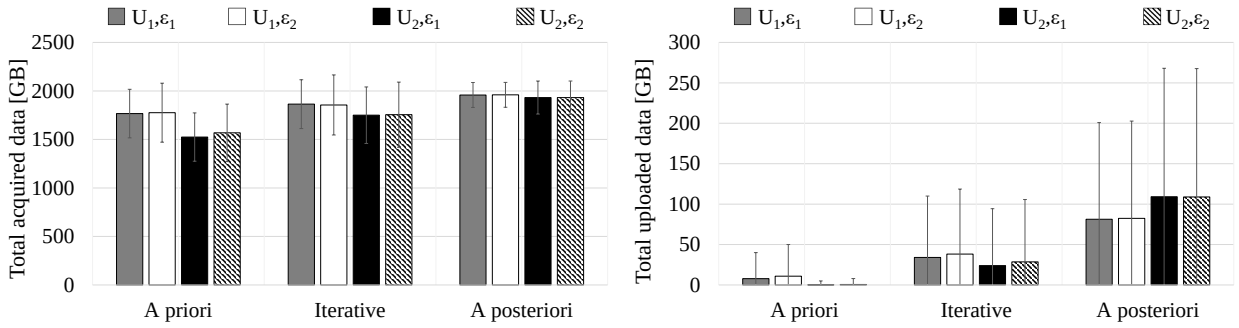

(a) Total acquired data. (b) Total uploaded data.

Fig. 6: Acquired and uploaded data in the 2048 GB configuration.

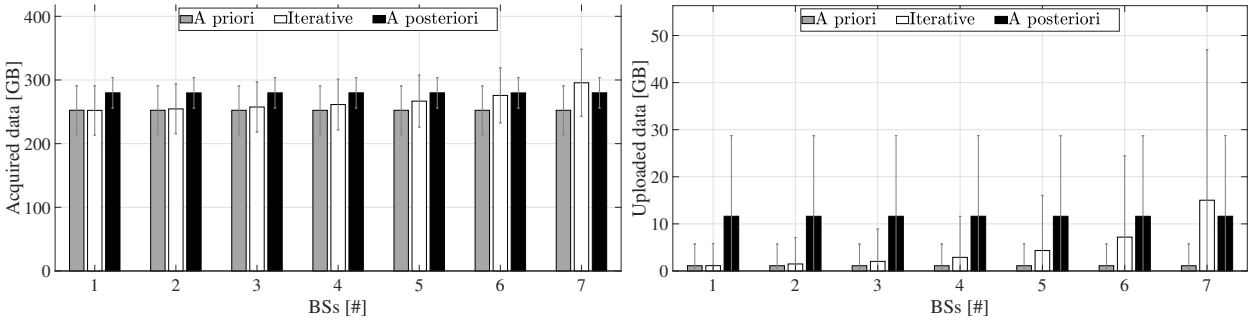

(a) Acquired data over each segment of an 7 CPs-long mission. (b) Uploaded data over each segment of an 7 CPs-long mission.

Fig. 7: Approaches Comparison in the 2048 GB configuration, with U_1, and ε_1.

and cooperative tasks optimization execution related problems. Second, the proposed approach could include trajectory design and path optimization. Thirdly, the 6G technological landscape can be further investigated to evaluate promising newbies, i.e., mmWaves.

ACKNOWLEDGMENTS

This work was partially supported by the Italian MIUR PON projects Pico&Pro (ARS01_01061), AGREED (ARS01_00254), FURTHER (ARS01_01283), RAFAEL (ARS01_00305) by Apulia Region (Italy) Research project INTENTO (36A49H6).

REFERENCES

[1] M. Gharibi, R. Boutaba, and S. L. Waslander, "Internet of drones," *IEEE Access*, vol. 4, pp. 1148–1162, 2016.

[2] A. Otto, N. Agatz, J. Campbell, B. Golden, and E. Pesch, "Optimization approaches for civil applications of unmanned aerial vehicles (uavs) or aerial drones: A survey," *Networks*, vol. 72, no. 4, pp. 411–458, 2018.

[3] L. Amorosi, L. Chiaraviglio, F. D'Andreagiovanni, and N. Blefari-Melazzi, "Energy-efficient mission planning of uavs for 5g coverage in rural zones," in *2018 IEEE International Conference on Environmental Engineering (EE)*, March 2018, pp. 1–9.

[4] M.Z. Chowdhury, M. Shahjalal, S. Ahmed, and Y.M. Jang, "6G wireless communication systems: Applications, requirements, technologies, challenges, and research directions.", *arXiv preprint arXiv:1909.11315*, 2019.

[5] Y. Zeng, J. Xu, and R. Zhang, "Energy minimization for wireless communication with rotary-wing uav," *IEEE Transactions on Wireless Communications*, vol. 18, no. 4, pp. 2329–2345, Apr. 2019.

[6] R. Citroni, F. Di Paolo, and P. Livreri, "A novel energy harvester for powering small uavs: Performance analysis, model validation and flight results," *Sensors*, vol. 19, pp. 173–184, 2019.

[7] Y. Zeng and R. Zhang, "Energy-efficient uav communication with trajectory optimization," *IEEE Transactions on Wireless Communications*, vol. 16, no. 6, pp. 3747–3760, Jun. 2017.

[8] A. Thibbotuwawa, P. Nielsen, B. Zbigniew, and G. Bocewicz, "Energy consumption in unmanned aerial vehicles: A review of energy consumption models and their relation to the uav routing," in *Information Systems Architecture and Technology: Proceedings of 39th International Conference on Information Systems Architecture and Technology – ISAT 2018*, 2019, pp. 173–184.

[9] L. Chiaraviglio, L. Amorosi, F. Malandrino, C. F. Chiasserini, P. Dell'Olmo, and C. Casetti, "Optimal throughput management in uav-based networks during disasters," in *IEEE INFOCOM 2019 - IEEE Conference on Computer Communications Workshops (INFOCOM WKSHPS)*, April 2019, pp. 307–312.

[10] A. S. Prasetia, R. Wai, Y. Wen, and Y. Wang, "Mission-based energy consumption prediction of multirotor uav," *IEEE Access*, vol. 7, pp. 33 055–33 063, 2019.

[11] S. Hayat, E. Yanmaz, T. X. Brown, and C. Bettstetter, "Multi-objective uav path planning for search and rescue," in *2017 IEEE International Conference on Robotics and Automation (ICRA)*, May 2017, pp. 5569–5574.

[12] T. Q. Duong, L. D. Nguyen, and L. K. Nguyen, "Practical optimisation of path planning and completion time of data collection for uav-enabled disaster communications," in *2019 15th International Wireless Communications Mobile Computing Conference (IWCMC)*, Jun. 2019, pp. 372–377.

[13] Q. Wu, L. Liu, and R. Zhang, "Fundamental trade-offs in communication and trajectory design for uav-enabled wireless network," *IEEE Wireless Communications*, vol. 26, no. 1, pp. 36–44, Feb. 2019.

[14] L. Li, X. Wen, Z. Lu, Q. Pan, and W. Hu, "Energy-efficient uav-enabled mec system: Bits allocation optimization and trajectory design," *Sensors*, vol. 19, pp. 1148–1162, October 2019.

[15] L. Xiao, Y. Liang, C. Weng, D. Yang, and Q. Zhao, "Uav-enabled data collection: Multiple access, trajectory optimization, and energy trade-off," *Wireless Communications and Mobile Computing*, vol. 2019, p. 14, 2019.

[16] G. Reina, A. Milella, R. Rouveure, M. Nielsen, R. Worst, and M. R. Blas, "Ambient awareness for agricultural robotic vehicles," *Biosystems Engineering*, vol. 146, pp. 114 – 132, 2016. [Online]. Available: http://www.sciencedirect.com/science/article/pii/S1537511015001889

[17] B. Prodanov, I. Kotsev, T. Lambev, L. Dimitrov, R. Bekova, and D. Dechev, "Drone-based geomorphological and landscape mapping of bolata cove, bulgarian coast," in *Proceedings of IMAM'2019 Congress*, 2019.

[18] M. Kulbacki, J. Segen, W. Knieć, R. Klempous, K. Kluwak, J. Nikodem, J. Kulbacka, and A. Serester, "Survey of drones for agriculture automation from planting to harvest," in *IEEE 22nd International Conference on Intelligent Engineering Systems (INES)*, June 2018, pp. 000 353–000 358.

[19] M. Zink, *Scalable Video on Demand: Adaptive Internet-based Distribution*. Wiley, October 2005.

[20] B. Fahs et al., "A meter-scale 600-Mb/s 2×2 imaging MIMO OOK VLC link using commercial LEDs and Si p-n photodiode array," 2017 26th Wireless and Optical Communication Conference (WOCC), Newark, NJ, 2017, pp. 1-6, doi: 10.1109/WOCC.2017.7928983.

[21] Intel Corporation, "Intel realsense technology d400 series product family," 1 2019. [Online]. Available: https://www.intel.com/content/dam/support/us/en/documents/emerging-technologies/intel-realsense-technology/Intel-RealSense-D400-Series-Datasheet.pdf

[22] DJI, "DJI Mavic 2 Tech Specs," 1 2020. [Online]. Available: https://www.dji.com/it/mavic-2/info#specs

[23] 3GPP, "Study on New Radio Access Technology Physical Layer Aspects (R. 14)," 3rd Generation Partnership Project, Tech. Rep. 38802, Sep 2017.